

Growth of *t*-Se Nanowires on the Surfaces of *a*-Se@Ag₂Se Core–Shell Particles through Controlled Release of Se from the *a*-Se Cores

Geon Dae Moon,[†] Unyong Jeong,^{*,†} and Younan Xia^{‡,§}

Department of Materials Science and Engineering, Yonsei University, 134 Shiinchon-dong, Seoul, Korea, Department of Chemistry, University of Washington, Seattle, Washington 98195-1700 (USA)

Received September 20, 2007

Revised Manuscript Received November 14, 2007

Most semiconductor 1D nanostructures with well-defined chemical composition and single crystallinity have been obtained via vapor phase routes.¹ Solution-based approaches have been mainly limited to the formation of zero-dimensional nanocrystals,² even though production of 1D nanostructures in solution may provide a more versatile route to semiconductor nanostructures in terms of cost and potential for large-scale production. Materials that intrinsically prefer anisotropic growth are ideal candidates for the synthesis of 1D nanostructures in a solution phase.³ Recent studies have demonstrated that trigonal selenium (*t*-Se) readily forms nanowires because of its strong tendency for anisotropic growth.⁴ The polymer-like bonding to form long and helical chains leads to an anisotropic growth for *t*-Se crystals. As a semiconductor, selenium has many important physical properties such as piezoelectricity, photoconductivity, thermoelectricity, and nonlinear optical responses.⁵ In recent years, *t*-Se has been synthesized as 1D nanostructures including nanowires, nanorods, nanobelts, and nanotubes through a

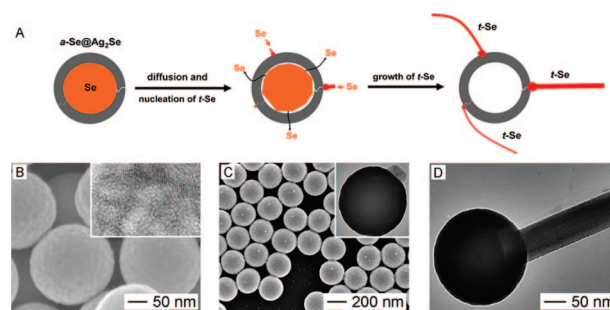


Figure 1. (A) Schematic illustrating the formation of *t*-Se nanowires from the surface of an *a*-Se@Ag₂Se core–shell colloidal sphere. (B) SEM image of *a*-Se@Ag₂Se core–shell particles; the inset shows a HR-TEM image of the Ag₂Se shell. The HR-TEM image shows the multiple grains in the shell. (C) SEM image displaying the nucleation of *t*-Se seeds on the particle surface, together with a TEM image at high magnification. (D) TEM image of a *t*-Se nanowire originating from the colloidal surface.

number of different methods that are based on solution-phase reactions.⁶ Xia and co-workers have also demonstrated the production of fine *t*-Se nanowires in bulk quantities using a sonochemical route.⁷ In related works, *t*-Se nanowires have been explored as chemical templates to obtain various chalcogenide nanowires.⁸ In this study, we demonstrate the formation of *t*-Se nanowires from *a*-Se@Ag₂Se core–shell particles in a controlled manner. To the best of our knowledge, there has been no report on the in situ growth of nanowires on the surface of a submicrometer-sized particle.

Figure 1A illustrates the growth mechanism, which involves the dissolution of *a*-Se core through cracks in the Ag₂Se shell, followed by nucleation and growth of *t*-Se nanowires on the particle surface. The polycrystalline nature of the Ag₂Se shell favors the formation of many types of defects such as vacancies, dislocations, grain boundaries, and cracks. Figure 1B gives a SEM and HR-TEM image of the particle surface, clearly showing the crystalline domains in the Ag₂Se shell. The enlarged HR-TEM image can be seen in the Supporting Information, Figure S-1. Both grain boundaries and cracks provide diffusion channels for Se atoms. As the dissolution of *a*-Se core proceeds, the grain boundaries can be supersaturated with the dissolved Se atoms. However, the narrow gap between the grains prohibits the formation of nuclei of *t*-Se. In contrast, cracks on the particle surface can provide sufficient spaces for the nucleation of *t*-Se nanocrystallites. The dissolved Se atoms can also nucleate heterogeneously on the surface of Ag₂Se shell to form *t*-Se seeds. These two nucleation mechanisms can take place simultaneously, and the exact probability may depend on the degree of supersaturation level of Se atoms

[†] Yonsei University.

[‡] University of Washington.

[§] Present address: Department of Biomedical Engineering, Washington University, St. Louis, MO 63130-4899.

- (1) (a) See recent reviews: Xia, Y.; Yang, P.; Sun, Y.; Wu, Y.; Mayers, B.; Gates, B.; Yin, Y.; Kim, F.; Yan, H. *Adv. Mater.* **2003**, *15*, 353. (b) Wang, F.; Dong, A.; Sun, J.; Tang, R.; Yu, H.; Buhro, W. E. *Inorg. Chem.* **2006**, *45*, 7511. (c) Fan, H. J.; Werner, P.; Zacharias, M. *Small* **2006**, *2*, 700.
- (2) (a) Peng, X.; Wickham, J.; Alivisatos, A. P. *J. Am. Chem. Soc.* **1998**, *98*, 7665. (b) Rogach, A. L.; Kornowski, A.; Gao, M.; Eychmuller, A.; Weller, H. *J. Phys. Chem. B* **1999**, *103*, 3065. (c) Muulec, F. V.; Kuno, M.; Bennati, M.; Hall, D. A.; Griffin, R. G.; Bawendi, M. G. *J. Am. Chem. Soc.* **2000**, *122*, 2532. (d) Talapin, D. V.; Rogach, A. L.; Kornowski, A.; Haase, M.; Weller, H. *Nano Lett.* **2001**, *1*, 207. (e) Li, L.-S.; Walda, J.; Manna, L.; Alivisatos, A. P. *Nano Lett.* **2002**, *2*, 557.
- (3) (a) Tang, Z.; Kotov, N. A.; Gierns, M. *Science* **2002**, *297*, 237. (b) Messer, B.; Song, J. H.; Huang, M.; Wu, Y.; Kim, F.; Yang, P. *Adv. Mater.* **2000**, *12*, 1526. (c) Ma, Y.; Qi, L.; Ma, J.; Cheng, H. *Adv. Mater.* **2004**, *16*, 1023. (d) Ma, Y.; Qi, L.; Shen, W.; Ma, J. *Langmuir* **2005**, *21*, 6161.
- (4) Mayers, B.; Gates, B.; Xia, Y. *Int. J. Nanotechnol.* **2004**, *1*, 86.
- (5) (a) Berger, L. I. *Semiconductor Materials*; CRC Press: Boca Raton, FL, 1997; p 86. (b) Chizhikov, D. M.; Shchastliviy, V. P. *Selenium and Selenides*; Colellets Publishing: London, 1968.
- (6) (a) Gates, B.; Yin, Y.; Xia, Y. *J. Am. Chem. Soc.* **2000**, *122*, 12582. (b) An, C.; Tang, K.; Liu, X.; Qian, Y. *Eur. J. Inorg. Chem.* **2003**, 3250. (c) Zhang, H.; Zuo, M.; Tan, S.; Li, G.; Zhang, S.; Hou, J. *J. Phys. Chem. B* **2005**, *109*, 10653. (d) Zhang, B.; Dai, W.; Ye, X.; Zuo, F.; Xie, Y. *Angew. Chem., Int. Ed.* **2006**, *45*, 2571. (e) Zhang, B.; Ye, X.; Dai, W.; Hou, W.; Zuo, F.; Xie, Y. *Nanotechnology* **2006**, *17*, 385. (f) Zhang, J.; Zhang; Sheng-Yi; Chen, H.-Y. *Chem. Lett.* **2004**, *33*, 1054.

- (7) (a) Gates, B.; Mayers, B.; Cattle, B.; Xia, Y. *Adv. Funct. Mater.* **2002**, *12*, 219. (b) Mayers, B. T.; Liu, K.; Sunderland, D.; Xia, Y. *Chem. Mater.* **2003**, *15*, 3852. (c) Gates, B.; Mayers, B.; Grossman, A.; Xia, Y. *Adv. Mater.* **2002**, *14*, 1749.

- (8) (a) Gates, B.; Wu, Y.; Yin, Y.; Yang, P.; Xia, Y. *J. Am. Chem. Soc.* **2001**, *123*, 11500. (b) Gates, B.; Mayers, B.; Wu, Y.; Sun, Y.; Cattle, B.; Yang, P.; Xia, Y. *Adv. Funct. Mater.* **2002**, *12*, 679. (c) Jiang, X.; Mayers, B.; Herricks, T.; Xia, Y. *Adv. Mater.* **2003**, *15*, 1740. (d) Jeong, U.; Xia, Y.; Yin, Y. *Chem. Phys. Lett.* **2005**, *416*, 246.

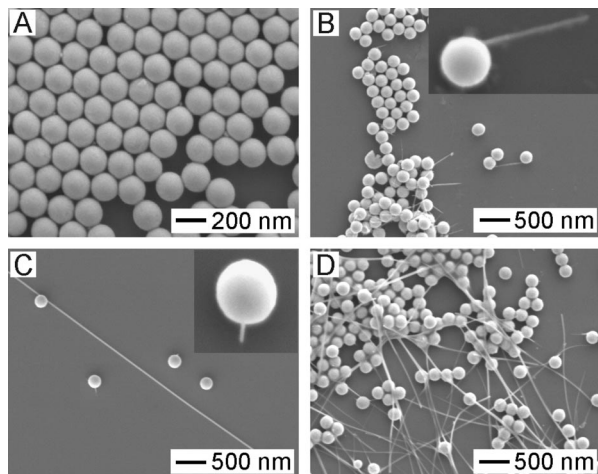


Figure 2. SEM images of (A) *a*-Se@Ag₂Se core-shell particles and (B–D) their temporal changes after being dispersed in ethanol at room temperature. (A) *a*-Se@Ag₂Se core-shell colloidal spheres; (B) short nanowires on a few colloidal particles after 24 h; (C) large length distribution of nanowires after 48 h; (D) long nanowires obtained after 6 days.

on the surface. The Se can be readily crystallized into a hexagonal lattice through van der Waals interactions. Crystallization of Se tends to occur along the *c*-axis, favoring the stronger covalent bonds over the relatively weak inter-chain van der Waals forces, which can make Se grow into 1D nanostructures.⁴ Figure 1C gives a SEM image of a sample obtained in the early stage of synthesis, clearly showing the formation of *t*-Se nanocrystallites on the surfaces of the core-shell particles. The nuclei on the surface can continuously grow as long as there is a supply of Se atoms from the amorphous core or from the solvent. Figure 1D shows a TEM image of a *t*-Se nanowire formed on the colloidal surface at the later stage of the synthesis.

The starting material, *a*-Se@Ag₂Se core-shell particles, was prepared by reacting monodisperse colloidal spheres of *a*-Se with AgNO₃ at room temperature.⁹ From EDX analysis developed in the previous work,⁹ the thickness of the Ag₂Se shell was estimated to be 20 nm. The transformation of *a*-Se@Ag₂Se was conducted in ethanol at room temperature without any agitation. Figure 2 shows a set of SEM images corresponding to samples obtained at different stages of *t*-Se nanowire growth: (A) premade *a*-Se@Ag₂Se colloids, (B) after 24 h, (C) after 48 h, and (D) after 6 days. Nanowires were observed only on the surfaces of the colloidal particles, indicating that homogeneous nucleation in the solution phase was not involved. As shown in Figure 2B, the number of *t*-Se nanowires on the surface of each colloidal particle was mostly limited to one or none. The slow dissolution of *a*-Se through cracks in the Ag₂Se shell kept the supersaturation of Se atoms on the surface at a low level. Although *t*-Se nanowires were successfully generated from the *a*-Se@Ag₂Se colloidal particles, their lengths showed a wide range of distribution as depicted in Figure 2C. This large length difference infers that the growth rate of nanowires is much higher than the rate of nucleation under the experimental conditions. The *t*-Se nanocrystals can nucleate at the colloidal surface via the supply of Se atoms from the Se core directly

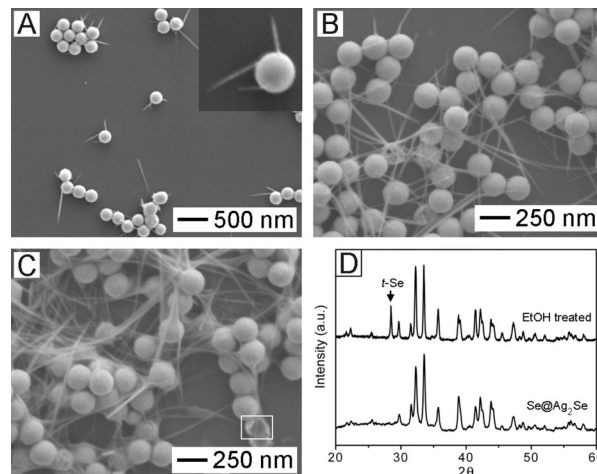


Figure 3. SEM images showing the formation of *t*-Se nanowires from *a*-Se@Ag₂Se colloidal particles in ethanol under continuous mild stirring at room temperature for different periods of time: (A) 17 h, (B) 24 h, and (C) 3 days. (D) XRD patterns taken from the as-synthesized *a*-Se@Ag₂Se core-shell particles and the same sample after it had been dispersed in ethanol for 3 days under magnetic stirring at room temperature.

to the defects on the surface or via diffusion of Se atoms dissolved in the solvent. The supply from the solvent should be the major source when the dissolution is fast because of mechanical stirring or thermal activation. In this case, the solution is homogenized and most *t*-Se nanocrystals nucleate evenly on all the colloidal surfaces. When the dissolution is not fast, a large fraction of nanocrystals nucleate in the defects on the surface. Some colloids without large defects on the surface fail to have a nucleation on the surface because the dissolved Se atoms are more likely consumed for the growth of existing nanocrystals on neighboring colloids.

The dissolution of Se cores in a solvent can be enhanced by mechanical stirring, which increases the supersaturation of Se and homogenizes the concentration in the solution. The high degree of supersaturation accelerates both the nucleation of *t*-Se seeds and their growth into nanowires. Figure 3 shows the formation of nanowires when the *a*-Se@Ag₂Se colloidal particles were dispersed in ethanol at room temperature under continuous mild stirring. In contrast to the results in Figure 2 that were obtained without stirring, 2–3 seeds nucleated on the surface of each colloidal particle and further grew as nanowires as shown in Figure 3A that was obtained after 17 h of reaction. The seeds grew much faster than those under no stirring. A larger amount of relatively long nanowires were obtained in 1 day (Figure 3B) and the growth was completed in 3 days (Figure 3C). The nanowires under continuous stirring had a much narrower length distribution than those obtained without stirring. The white box in Figure 3C highlights a broken colloidal particle, showing the hollow interior after complete consumption of *a*-Se cores. X-ray diffraction patterns in Figure 3D confirmed that the nanowires grown from the *a*-Se@Ag₂Se colloids had been crystallized into the pure trigonal phase.

The dissolution of Se should be accelerated as the solution temperature increases. Figure 4A shows *t*-Se nanowires grown from *a*-Se@Ag₂Se colloidal particles dispersed in ethanol at 60 °C. The reaction was allowed for 3 days under

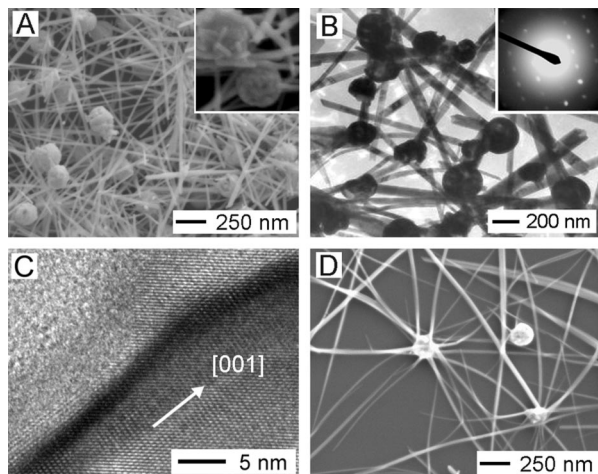


Figure 4. SEM and TEM images showing the formation of *t*-Se nanowires at 60 °C under continuous stirring in different solvents for different periods of time: (A–C) ethanol (1 day) and (D) isopropanol (1 day).

continuous stirring. The transformation from *a*-Se to *t*-Se could be completed within 1 day, which is much faster than the synthesis at room temperature. The nanowires obtained at 60 °C were relatively thicker than those grown at room temperature. The enhanced dissolution of Se increased the number of *t*-Se nanowires on the surface of each colloidal particle and reduced the length distribution. The inset of Figure 4A shows that 6–7 or more *t*-Se seeds nucleated on the surface of each colloidal particle. The Ag₂Se shells were contracted as the Se core were dissolved, which indicates decreased modulus of the shells at 60 °C. An enlarged image showing the collapsed shells is shown in the Supporting Information, Figure S-2. From the TEM image and diffraction pattern in Figure 4B, the nanowires were characterized as single crystals with the uniform lateral dimension. The HR-TEM image in Figure 4C shows the growth of nanowires along the $\langle 001 \rangle$ direction of the hexagonal lattice.

For the synthesis of *t*-Se nanowires, it is critical to select an appropriate solvent in which *a*-Se is soluble but *t*-Se is insoluble. Such solvents can allow the nucleation of *t*-Se and the continuous deposition of Se atoms from the solution onto the *t*-Se seeds. Primary alcohols with short chains have been known to produce high-quality long *t*-Se nanowires, whereas those with long alkyl chains deteriorates the quality of nanowires.^{7b} We compared the morphology of the *t*-Se nanowires obtained from ethanol and 2-propanol. Figure 4D shows SEM image of *t*-Se nanowires grown in 2-propanol at 60 °C under continuous magnetic stirring for 3 days. There are as many nanowires as in the sample obtained in ethanol at 60 °C. The tapered nanowires could be easily observed in this study, as shown in Figure 4C. The nanowires grown in 2-propanol were thicker and longer than those produced in ethanol. The tapering mechanism for the *t*-Se nanowires is yet to be investigated. When the colloidal

particles were dispersed in water and kept at 60 °C under continuous stirring for 3 days, 1–2 small dots were formed on the particle surface instead of nanowires. The Supporting Information, Figure S-3, shows a SEM image with a blow-up TEM image in the inset. The substantially reduced solubility of Se in water are considered to prohibit the formation of nanowires. Although Se atoms may diffuse out through cracks and then *t*-Se seeds are formed on the surface, the supply of Se atoms from the solution was not enough for the growth of seeds into nanowires.

In summary, we have presented a method for growing nanowires on the surfaces of micrometer-sized colloidal particles. This approach can be readily applied to materials that are in a less stable state and favor anisotropic growth. In this study, we demonstrated the growth of single-crystal *t*-Se nanowires on the surfaces of *a*-Se@Ag₂Se core-shell colloidal particles through controlled release of Se from the core. The number of nanowires on the surface and their thickness could be controlled by adjusting the solubility of Se in the solvent. The heterostructure—Ag₂Se hollow particle with *t*-Se nanowires attached to its surface—can be transformed into different materials by employing it as a physical or chemical template. For example, metal coating can produce pinlike metal tubes by employing the previously reported procedures.¹⁰ Chemical transformation of *t*-Se nanowires has been known to produce various chalcogenide nanowires and nanotubes such as Ag₂Se and CdSe.^{8d} By using cation-exchange reactions, the Ag₂Se colloidal part can be transformed into other chalcogenide semiconductors such as CdSe, PbSe, and ZnSe.¹¹ This will allow us to bring more morphological and compositional variations to 1D nanostructures, enabling the fabrication of functional devices. In addition, the use of ambient conditions, mild solvents, and relatively low temperatures (<60 °C) should allow us to scale-up this synthesis for large-scale production.

Acknowledgment. This work was supported in part by the Korea Research Foundation Grant funded by the Korean Government (MOEHRD) (KRF-2006-311-D00411) and the Seoul R&BD Program (10816). U.J. thanks the NGNT project (No. 10024135-2005-11) from the Korean Ministry of Commerce, Industry and Energy (MOCIE).

Supporting Information Available: SEM and TEM images showing the crystal domains of Ag₂Se shell surface, collapsed Ag₂Se shell after annealing at 60 °C in ethanol, and the result in water (PDF). The information is available free of charge via the Internet at <http://pubs.acs.org>.

CM702695U

- (10) (a) Mayers, B.; Jiang, X.; Sunderland, D.; Cattle, B.; Xia, Y. *J. Am. Chem. Soc.* **2003**, *125*, 13364. (b) Jeong, U.; Herricks, T.; Shahar, E.; Xia, Y. *J. Am. Chem. Soc.* **2005**, *127*, 1098.
 (11) Camargo, P. H. C.; Lee, Y. H.; Jeong, U.; Zou, Z.; Xia, Y. *Langmuir* **2007**, *23*, 2985.